
Causal Fairness for Survival Analysis

Drago Plečko

Department of Statistics & Data Science
UCLA

Abstract

In the data-driven era, large-scale datasets are routinely collected and analyzed using machine learning (ML) and artificial intelligence (AI) to inform decisions in high-stakes domains such as healthcare, employment, and criminal justice, raising concerns about the fairness behavior of these systems. Existing works in fair ML cover tasks such as bias detection, fair prediction, and fair decision-making, but largely focus on static settings. At the same time, fairness in temporal contexts, particularly survival/time-to-event (TTE) analysis, remains relatively underexplored, with current approaches to fair survival analysis adopting statistical fairness definitions, which, even with unlimited data, cannot disentangle the causal mechanisms that generate disparities. To address this gap, we develop a causal framework for fairness in TTE analysis, enabling the decomposition of disparities in survival into contributions from direct, indirect, and spurious pathways. This provides a human-understandable explanation of why disparities arise and how they evolve over time. Our non-parametric approach proceeds in four steps: (1) formalizing the necessary assumptions about censoring and lack of confounding using a graphical model; (2) recovering the conditional survival function given covariates; (3) applying the Causal Reduction Theorem to reframe the problem in a form amenable to causal pathway decomposition; (4) estimating the effects efficiently. Finally, our approach is used to analyze the temporal evolution of racial disparities in outcome after admission to an intensive care unit (ICU).

1 Introduction

Large-scale data collection and analysis is increasingly changing decision-making in a variety of real-world settings. Datasets capturing information from hiring processes, university admissions, law enforcement, credit lending and loan approvals, health care interventions, and other high-stakes domains are now routinely processed using machine learning and artificial intelligence to inform or automate decisions [19, 25, 7, 38]. In this context, society is increasingly concerned about how the nature, scope, and quality of these datasets, combined with algorithmic analysis, may shape the future world in which existing decision processes are automated. Prior works highlight that data-driven systems can perpetuate or even amplify inequities between demographic groups, with documented examples in criminal justice [2], computer vision [8], and online advertising [42, 13], to cite a few. More recently, similar concerns have emerged in generative AI [15]. Notably, however, the new data-driven era has also highlighted the fact that inequities are pervasive when decisions are made by humans, and the datasets recording these decisions often encode historical biases. Well-known examples in the literature include the gender pay gap [4, 5] and racial bias in criminal sentencing [43, 29]. As a result, data collected from the current reality will encode these patterns, effectively embedding past discriminatory decisions against certain protected groups. Naturally, predictive or generative models developed on such data are at risk of exhibiting undesirable bias. These observations gave rise to the growing field of fair machine learning, although as described above, many core issues originate before ML systems are even deployed.

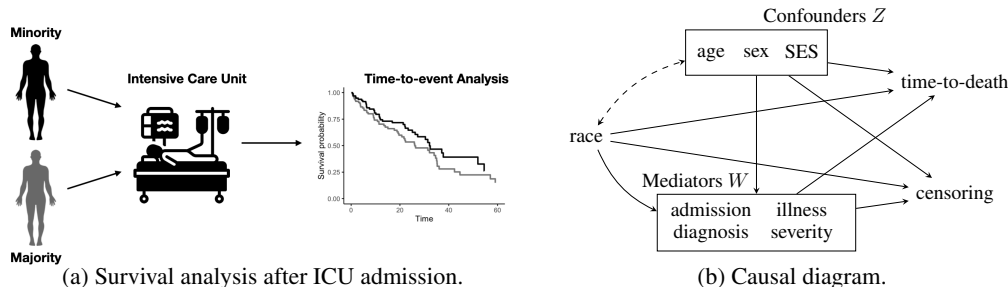


Figure 1: Introductory example of race differentials after intensive care unit (ICU) admission.

Within this context, it is useful to distinguish between different tasks appearing in the growing literature on fair ML. One can identify three specific and distinct tasks: (1) bias detection and quantification for existing outcomes or decision policies; (2) construction of fair predictions of an outcome; and (3) construction of fair decision-making policies intended for real-world implementation [33]. An additional helpful distinction is between static and dynamic fairness settings, which interacts with the above-mentioned tasks. In the former, the goal is to analyze a *snapshot* of reality at a single time point. In the latter, the objective is to understand how disparities between groups emerge and evolve over time. Dynamic, time-resolved settings arise naturally when institutions repeatedly evaluate cohorts, such as in hiring or college admission decisions. In some cases, the same cohort of individuals may be subject to sequential decisions, or the focus may be on the time elapsed before an event occurs, with attention to group differences. This final case, involving time-to-event (TTE) or survival analysis, is the focus of this paper.

While a flurry of recent work focuses on fairness [31], most commonly in static settings concerning fair prediction, some areas in the fair ML landscape remain relatively understudied, particularly those involving temporal data. Existing works on fairness in TTE analysis primarily adopt statistical definitions of fairness [40, 35, 16, 45], which, on their own, cannot distinguish between different causal mechanisms that generate disparity in the real world, even with unlimited data. For this reason, a field studying fairness through a causal lens has emerged [22, 46, 11, 33], enabling human-understandable and interpretable definitions and metrics of fairness that are explicitly tied to the causal mechanisms transmitting change between groups. Within the literature on causal fairness, however, few dynamic settings have been investigated, with some notable exceptions [27, 12]. Thus, within the causal approach, there remains a need for a deeper understanding of how causal reasoning can be applied to fairness in temporal data, such as TTE analysis.

In this work, our aim is to fill this gap, and offer a principled approach for causal fairness analysis in TTE settings. We next describe the motivating example studied in the paper:

Example 1 (Time-to-Death Differentials after ICU). *Patients are admitted to an intensive care unit (ICU) for various life-threatening conditions. Upon admission, patient data is collected, including admission diagnosis and illness severity information (W), as well as demographic information such as age and socioeconomic status (Z). The outcome of interest is the time to death after ICU admission (T), and the study aims to compare groups defined by race (X). Fig. 1a provides an overview.*

In the data, instead of directly observing the true time to death T , we observe the patient’s study end time M and a censoring indicator δ . If $\delta = 0$, M corresponds to a censoring time (the patient is removed from the study and no longer observed), while $\delta = 1$ implies that M equals the death time T . The exact censoring mechanism depends on the study design and data availability.

The causal diagram in Fig. 1b illustrates that the attribute X may influence the time to death T through multiple causal pathways: direct path ($X \rightarrow T$), indirect path ($X \rightarrow W \rightarrow T$), and spurious (confounded) path ($X \leftrightarrow Z \rightarrow T$). While a typical static analysis might examine the direct, indirect, and spurious effects of race on in-hospital mortality (or mortality within a fixed time window), our goal is to explain, in a time-dependent fashion, how disparities in survival evolve. \square

Specifically, the contributions of the paper are the following:

- (i) We formalize causal fairness in survival analysis and prove the Causal Reduction Theorem (Thm. 1), allowing us to identify and decompose group disparities in TTE settings.

- (ii) We instantiate the framework in three regimes: non-informative censoring (Sec. 2), competing risks (Sec. 2.1), and informative censoring (Sec. 2.2). We derive identification results for each of the settings (Prop. 1).
- (iii) We prove two new technical results: a doubly robust estimator for censored data (Thm. 2), and sharp bounds for copula-graphic estimation under non-disjoint increments (Thm. 3).
- (iv) We analyze race differentials in post-ICU mortality, demonstrating that causal fairness for TTE yields scientific insights missed by standard statistical fairness analyses.

1.1 Related Work

Some previous works investigate fairness notions for TTE analysis [40, 35, 16]. These studies focus on statistical definitions of fairness for quantifying disparities, whereas our goal is to develop and apply causal notions of fairness. Our work is also connected to the literature on causal fairness [46, 33] that introduces important causal fairness notions, but is concerned with the static setting only, while we extend these ideas to the context of TTE analysis. Another work related to ours is [32], which provides a causal-inspired fairness discussion in a TTE setting, although a statistical notion of fairness is adopted therein. Finally, our work is related to the literature on causal mediation for survival analysis [23, 44]. However, most of this literature adopts parametric models, often specifying particular forms for the survival time or mediator distributions. By contrast, we focus on non-parametric inference, avoiding strong modeling assumptions about the distributional form of survival times or mediators.

1.2 Preliminaries

We use structural causal models (SCMs) as our semantical framework [30]. An SCM is a tuple $\mathcal{M} := \langle V, U, \mathcal{F}, P(u) \rangle$, where V, U are sets of endogenous (observable) and exogenous (latent) variables respectively, \mathcal{F} is a set of functions f_{V_i} , one for each $V_i \in V$, where $V_i \leftarrow f_{V_i}(\text{pa}(V_i), U_{V_i})$ for some $\text{pa}(V_i) \subseteq V$ and $U_{V_i} \subseteq U$. $P(u)$ is a strictly positive probability measure over U . Each SCM \mathcal{M} is associated with a causal diagram \mathcal{G} over the nodes V , where $V_i \rightarrow V_j$ if V_i is an argument of f_{V_j} , and $V_i \leftrightarrow V_j$ if the corresponding U_{V_i}, U_{V_j} are not independent. An instantiation of the exogenous $U = u$ is called a *unit*. By $Y_x(u)$ we denote the potential response of Y when setting $X = x$ for the unit u , which is the solution for $Y(u)$ to the set of equations obtained by evaluating the unit u in the submodel \mathcal{M}_x , in which all equations in \mathcal{F} associated with X are replaced by $X = x$.

2 Causally Fair Survival – Non-Informative Censoring

Our first step is to conceptualize the notions of causal fairness in the context of survival analysis. We assume access to a specific cluster causal diagram \mathcal{G}_{SFM} known as the standard fairness model (SFM) [33], which we adapt to the setting of survival analysis. The SFM (Fig. 2a) consists of the following: *protected attribute*, labeled X (e.g., gender, race, religion), assumed to be binary; the set of *confounding* variables Z , which are not causally influenced by the attribute X (e.g., demographic information, zip code), but could share co-variations with X ; the set of *mediator* variables W that are possibly causally influenced by the attribute.

Further, the variable T denotes the survival time of the individual for the specific event of interest, while C denotes the time to censoring. These variables are in a shaded gray area, since they are assumed not to be observed. Instead, we observe the pair (M, δ) , where $M = \min\{T, C\}$ and $\delta = \mathbb{1}(T \leq C)$ is the indicator of whether the observed event is death or not.

The SFM in Fig. 2a encodes some important assumptions for our analysis, which can be broken into two parts. Firstly, the graphical model implies that variables T, C are independent conditional on X, Z, W , written as $T \perp\!\!\!\perp C \mid X, Z, W$, since there is no unobserved confounding between T and C (absence of a bidirected arrow $T \leftrightarrow C$). This assumption, which stipulates that the censoring mechanism is (conditionally) independent of the survival mechanism, allows the application of the standard tools of survival analysis, such as the (conditional) Kaplan-Meier [18] or Nelson-Aalen [28, 1] estimators. This assumption requires careful justification, and can often be used when the censoring occurs due to administrative reasons such as study termination (violations of this assumption are discussed in Sec. 2.2). The second part of the assumptions relates to the lack-of-confounding assumptions typically used in the causal inference literature. In particular, note that there are no

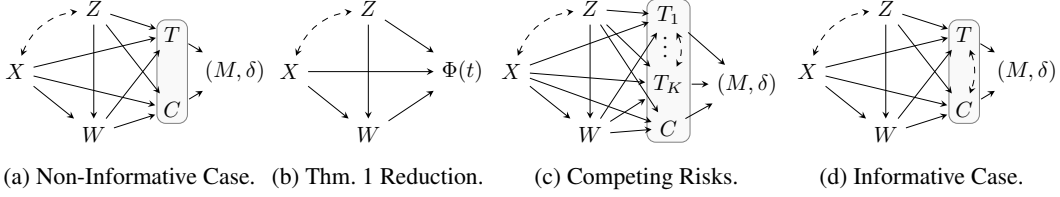


Figure 2: Standard Fairness Models for different settings.

bidirected edges between sets $\{T, C, M, \delta\}$ and $\{X, Z, W\}$, and also there are no bidirected arrows between X, W or Z, W . These lack-of-confounding assumptions (encoded through absences of bidirected edges) are important for identification of different effects of the attribute X on the survival curve. The above two sets of assumptions also correspond to the steps of our analysis in the sequel.

Our goal is to explain any observed discrepancies between the survival curves for the demographic groups $X = x_0$ (e.g., male) and $X = x_1$ (e.g., female). In particular, we are interested in explaining survival differences, measured by the so-called total variation measure $\text{TV}_{x_0, x_1}(t)$:

$$P(T > t | X = x_1) - P(T > t | X = x_0) \quad (1)$$

across time points $t \in [0, \infty)$. The survival curve $P(T > t)$ will be denoted by $S(t)$, and the conditional by $S(t | x)$. We aim to decompose the measure of disparity in Eq. 1 into the contributions of (a) the direct effect, along the arrow $X \rightarrow T$; (b) indirect effect $X \rightarrow W \rightarrow T$; and (c) spurious/confounded effect $X \leftrightarrow Z \rightarrow T$. For decomposing the measures, we will follow a two-step process, which is closely related to the two types of assumptions encoded in the SFM in Fig. 2a. The first step is related to inference of $P(T | X, Z, W)$, whereas the second step is related to inference of causal effects of X on functionals of $P(T | X, Z, W)$, once the conditional distribution of the survival time $P(T | X, Z, W)$ has been established.

Step 1: Inferring $P(T | X, Z, W)$ The first challenge is related to the inference of the distribution $P(T | X, Z, W)$ only from data on (X, Z, W, M, δ) . As mentioned earlier, the core challenge stems from the fact that variables T, C remain unobserved (the variables in shaded area in Fig. 2a). Instead, we have access to the pair (M, δ) , and depending on the censoring mechanism, inference of $P(T | X, Z, W)$ may or may not be possible. Under the assumption $T \perp\!\!\!\perp C | X, Z, W$ encoded in Fig. 2a, however, the likelihood for T is a function of (M, δ) alone, and conditional Kaplan-Meier (for survival) and Nelson-Aalen (for cumulative hazard) are valid.

Step 2: Inference of Causal Effects on ϕ . We next assume $P(T | X, Z, W)$ is known, and define $\Phi \triangleq \phi(P(T | X, Z, W))$, where Φ depends on the random values of X, Z, W , whereas ϕ is a mapping from the space of conditional distributions of T into \mathbb{R} . Eq. 1 can thus be written as

$$\mathbb{E}[\Phi | X = x_1] - \mathbb{E}[\Phi | X = x_0], \quad (2)$$

where $\Phi(t) = P(T > t | X, Z, W)$. This observation, that $\Phi(t)$ is obtained by applying a known transformation ϕ to an identifiable distribution $P(T | X, Z, W)$, allows us to construct another causal model, as described in the following result (all proofs are in Sec. A):

Theorem 1 (Reduced Standard Fairness Model). *Let \mathcal{M} be an SCM compatible with the SFM in Fig. 2d. Let ϕ be a functional mapping $P(T | X, Z, W)$ to \mathbb{R} . The structural mechanism of the random variable Φ is then given by:*

$$f_{\Phi}(x, z, w) = \phi(P(T | X = x, Z = z, W = w)). \quad (3)$$

Therefore, the variable Φ is a deterministic function of X, Z, W , not depending on any of the noise variables U , and we can add Φ to the causal diagram as in Fig. 2b.

The above theorem is quite helpful as it allows us to establish the causal diagram for the new variable $\Phi(t)$. Then, we consider the notions of direct, indirect, and spurious effects: $x\text{-DE}_{x_0, x_1}(\Phi | x) = \mathbb{E}[\Phi_{x_1, W_{x_0}} | x] - \mathbb{E}[\Phi_{x_0} | x]$, $x\text{-IE}_{x_1, x_0}(\Phi | x) = \mathbb{E}[\Phi_{x_1, W_{x_0}} | x] - \mathbb{E}[\Phi_{x_1} | x]$, and $x\text{-SE}_{x_1, x_0}(\Phi) = \mathbb{E}[\Phi_{x_1} | x_0] - \mathbb{E}[\Phi_{x_1} | x_1]$. Based on these, the $\text{TV}_{x_0, x_1}(\Phi)$ measure $\mathbb{E}[\Phi | X = x_1] - \mathbb{E}[\Phi | X = x_0]$ can be decomposed as [46, 33]:

$$\text{TV}_{x_0, x_1}(\Phi) = x\text{-DE}_{x_0, x_1}(\Phi | x_0) - x\text{-IE}_{x_1, x_0}(\Phi | x_0) - x\text{-SE}_{x_1, x_0}(\Phi). \quad (4)$$

The x -DE measures the contribution of an $x_0 \rightarrow x_1$ transition along the direct $X \rightarrow \Phi$ path; the x -IE and x -SE measure the reverse $x_1 \rightarrow x_0$ transition along the indirect $X \rightarrow W \rightarrow \Phi$ and spurious $X \leftarrow Z \rightarrow \Phi$ paths, respectively [33]. From these, Eq. 4 decomposes the marginal Φ -disparity into causal pathway contributions, while Thm. 1 allows us to do this at each time point. Furthermore, under the SFM in Fig. 2b, these effects are identifiable from observational data:

Proposition 1 (Identification of Causal Effects). *Let \mathcal{M} be an SCM compatible with the Standard Fairness Model, and let $P(V)$ be its observational distribution. The potential outcome $\mathbb{E}[\Phi_{x_y, W_{x_w}}(t) | X = x_z]$ can be identified as:*

$$\sum_{z, w} \mathbb{E}[\Phi(t) | x_y, z, w] P(W = w | X = x_w, Z = z) P(Z = z | X = x_z). \quad (5)$$

Prop. 1 gives us a way to identify a generic potential outcome $\mathbb{E}[\Phi_{x_y, W_{x_w}}(t) | X = x_z]$ of the survival function in the counterfactual world where $X = x_y$ along the direct, $X = x_w$ along the indirect, and $X = x_z$ along the spurious path. For estimating the causal effects on RHS of Eq. 4, different choices of $x_y, x_w, x_z \in \{0, 1\}$ need to be used as appropriate. The above identification results allows us to identify key causal fairness quantities in a TTE setting with non-informative censoring. We next discuss how to estimate the target quantities in practice using either (1) model-based estimation or (2) doubly-robust estimation.

Model-Based Estimation. Given our interest in mixed data types with varying dimension, and non-parametric inference, we use random survival forests (RSF) [17] for estimating $P(T | X, Z, W)$. RSF estimates the conditional cumulative hazard function $\Lambda(t | X, Z, W)$, by averaging the Nelson-Aalen estimator of the CHF across the leaf nodes of different trees. From $\Lambda(t | X, Z, W)$, the survival function is easily obtained via $S(t | X, Z, W) = \exp(-\Lambda(t | X, Z, W))$, allowing effect estimation:

Proposition 2 (Model-Based Estimation of Causal Effects). *Denote by $f(x, z, w)$ the estimator of $\mathbb{E}[\Phi | x, z, w]$, and by $\hat{P}(x | v')$ the estimator of the probability $P(x | v')$ for different choices of v' . The potential outcome $\mathbb{E}[\Phi_{x_y, W_{x_w}}(t) | X = x_z]$ can be estimated as:*

$$\frac{1}{n} \sum_{i=1}^n f(x_y, z_i, w_i) \frac{\hat{P}(x_w | z_i, w_i)}{\hat{P}(x_w | z_i)} \frac{\hat{P}(x_z | z_i)}{\hat{P}(x_z)}. \quad (6)$$

Prop. 2 provides us with a basis for model-based estimation of causal effects (as opposed to doubly-robust estimation discussed in the sequel). As mentioned earlier, the Φ variable can be thought of as time-dependent. In our setting, where X, Z, W that do not vary over time, the estimated propensities $\hat{P}(x | v')$ also do not depend on time, implying that the time component of the causal decomposition is obtained in a computationally inexpensive way.

Doubly-Robust Estimation. Our second approach is based on doubly-estimation of causal effects [3]. We prove a new technical result for doubly-robust estimation of counterfactual effects based on censored data, by using the appropriate influence function for debiasing the model-based estimator:

Theorem 2 ($\Phi(t)$ Potential Outcome Influence Function). *Let ψ denote the potential outcome $\mathbb{E}[\Phi_{x_y, W_{x_w}}(t) | X = x_z]$. Then, the influence function for ψ , written $\mathbb{IF}(\psi)$, is given by:*

$$\begin{aligned} & \frac{\mathbb{1}(X = x_y) \lambda_{x_z, x_w}(Z)}{P(x_z) \lambda_{x_y, x_w}(Z, W)} \left[\frac{\mathbb{1}(M > t)}{G(t | X, Z, W)} + \xi_1(t) - \xi_2(t) - S(x_y, Z, W) \right] \\ & + \frac{\mathbb{1}(X = x_w)}{P(x_z) \lambda_{x_w, x_z}(Z)} [S(x_y, Z, W) - \nu_{x_y, x_w}(Z)] + \frac{\mathbb{1}(X = x_z)}{P(x_z)} [\nu_{x_y, x_w}(Z) - \psi], \end{aligned} \quad (7)$$

where $G(t | X, Z, W) = P(C > t | X, Z, W)$, $S(x, Z, W) = S(t | x, Z, W)$, $\lambda_{x_a, x_b}(V) = \frac{P(x_a | V)}{P(x_b | V)}$, $\nu_{x_a, x_b}(Z) = \mathbb{E}[S(x_a, Z, W) | x_b, Z]$, $\xi_1(t) = \frac{\mathbb{1}(M \leq t, \delta = 0) S(t | X, Z, W)}{S(M | X, Z, W) G(M | X, Z, W)}$, and $\xi_2(t) = S(t | X, Z, W) \int_0^t \frac{\mathbb{1}(M \geq u) h_C(u | X, Z, W)}{S(u | X, Z, W) G(u | X, Z, W)} du$, where h_C is the conditional censoring hazard.

The proof of the theorem, together with a further discussion on the details of doubly robust estimation, is provided in Sec. C. We estimate ψ using cross-fitting [10]: nuisance functions G, S and propensities are fitted on one fold (via xgboost [9]), while the IF is evaluated on the remaining data, and folds are swapped in turn to obtain the final one step debiased estimate.

2.1 Causal Fairness under Competing Risks

While the Cond-NIC setting considered so far is the most commonly studied scenario in TTE analysis [20], a wide range of real-world applications require moving beyond this basic case. In particular, individuals may often be simultaneously at risk of multiple, distinct event types, all of which are of interest to us. This leads to the setting of *competing risks* (CR).

Formally, in the CR setting (see Fig. 2c), each individual is at risk of K event types, indexed by $J \in \{1, \dots, K\}$. Let T_k denote the unobserved time to event of type k , and let C denote the time to censoring. Available to us are only

$$M = \min\{T_1, \dots, T_K, C\}, \quad \delta \in \{0, 1, \dots, K\}, \quad (8)$$

where $\delta = k$ indicates that event k occurred at time M , and $\delta = 0$ indicates censoring. As in Sec. 2, censoring is assumed to be conditionally independent of the event process, $C \perp\!\!\!\perp (T_1, \dots, T_K) \mid X, Z, W$. A key feature of the competing risks setting is that all event types are of interest, rather than some being treated as nuisances. While it is conceptually appealing to model the full joint distribution $P(T_1, \dots, T_K \mid X, Z, W)$, this is generally infeasible from observed data, since only the minimum event time is observed, and the competing events may have unobserved common causes (bidirected edges among T_1, \dots, T_K in Fig. 2c). Therefore, identification of the joint distribution would require strong additional assumptions, such as independence of failure times, which rarely holds. As a result, most approaches to competing risks focus on functionals of the observable process, most commonly cause-specific hazards [14] or cumulative incidence functions (CIFs) [20]. In this work, we focus on the latter. For cause k , the cumulative incidence function is defined as

$$\text{CIF}_k(t \mid X, Z, W) = P(T_k \leq t, T_k \leq \min_j T_j \mid X, Z, W). \quad (9)$$

The CIF is simply the proportion of individuals who experience event k by time t . Importantly, CIFs explicitly account for competition between event types: increasing the rate of one event type necessarily reduces the CIFs of the remaining events. Indeed, letting

$$S_{\text{all}}(t) = P(\min\{T_1, \dots, T_K\} > t) \quad (10)$$

denote the all-cause (event-free) survival function, we have $\sum_{k=1}^K \text{CIF}_k(t) = 1 - S_{\text{all}}(t)$. This behavior differs from quantities such as $P(T_k > t \mid X, Z, W)$, which do not reflect the presence of competing events. These nuances need to be taken into account when interpreting causal fairness decompositions in the CR setting, where CIFs are treated as the outcome of interest. Specifically, for each cause k and time point t , we define

$$\Phi_k(t) \triangleq \text{CIF}_k(t). \quad (11)$$

By Thm. 1, each $\Phi_k(t)$ is a deterministic functional of $P(T_1, \dots, T_K \mid X, Z, W)$, and hence a deterministic function of (X, Z, W) . This again induces a reduced causal model in which X, Z , and W influence $\Phi_k(t)$ (Fig. 2b). Our analysis proceeds by quantifying, for each event type k , the x -specific direct, indirect, and spurious effects of X on $\text{CIF}_k(t)$. Intuitively, these effects describe how changes in the protected attribute X along different causal pathways influence the cumulative incidence of event k over time. In addition, we also quantify the corresponding effects on the all-cause survival function $S_{\text{all}}(t)$, thereby providing both cause-specific and aggregate perspectives on survival disparities. Regarding estimation, we can again either follow a model-based or a doubly-robust approach. A discussion of estimation in the CR setting, including the derivation of influence functions for CIFs, is given in Sec. C.

2.2 Causal Fairness under Informative Censoring

The third and final setting we consider is that of *informative censoring* (IC). This setting is very common in real-world data and arises when the mechanism by which individuals are censored carries information about the event of interest. Another common setting where informative censoring occurs is when multiple terminal events are possible, but we are interested in analyzing just one of them. Formally, in the IC setting, we consider an outcome with event time T and a censoring time C that is informative about T . Unlike the settings of NIC (Sec. 2) and CR (Sec. 2.1), we no longer assume that $T \perp\!\!\!\perp C \mid X, Z, W$ (see Fig. 2d where there is a bidirected arrow $T \leftrightarrow C$). As a result, standard tools from survival analysis are not directly applicable. The object of interest in this setting

is typically the survival function $S(t | X, Z, W) = P(T > t | X, Z, W)$. Specifically, in our running example, one may be interested in time-to-readmission to ICU in a world where death does not exist as a competing risk. As discussed previously, inference of such quantities is not possible without additional assumptions. Therefore, to proceed, we adopt a sensitivity analysis approach based on assumptions about the joint law of (T, C) . Specifically, we assume that the joint survival function $H(t, c) = P(T > t, C > c)$ is described by an Archimedean copula

$$H(t, c) = \mathcal{C}_\tau(S(t), G(c)) \quad (12)$$

parameterized by Kendall's τ , which is our sensitivity parameter. Let φ be the generator function of the copula, which is typically decreasing and convex. By definition, Eq. 12 implies the relationship

$$\varphi(H(t, c)) = \varphi(S(t)) + \varphi(G(c)), \quad (13)$$

where $S(t) = P(T > t)$ and $G(c) = P(C > c)$ denote the survival functions of T and C .

Copula-Graphic Estimation. The copula-graphic estimator (CGE) exploits the relationship in Eq. 13 to recover the marginal survival functions $S(t)$ and $G(c)$ from observable quantities. In the classical CGE setting, time is discretized on a grid $\{t_1, \dots, t_m\}$, and it is assumed that at each grid point only one of $S(t)$ or $G(t)$ exhibits a jump, with both functions being piecewise constant. Under these assumptions, $S(t)$ and $G(t)$ can be recursively identified from the estimable $\text{CIF}_T(t)$, $\text{CIF}_C(t)$ of T, C . This approach is known as the CGE [6]. In our setting, however, estimation proceeds on a fixed grid of estimated CIFs, and we cannot assume that only one of $\hat{S}(t_i)$ or $\hat{G}(t_i)$ jumps at a given grid point. Consequently, the classical CGE must be adapted: the copula parameter τ no longer uniquely identifies $\hat{S}(t_{i+1})$ and $\hat{G}(t_{i+1})$ from the estimated CIFs, but identifies their bounds:

Theorem 3 (CGE bounds under non-disjoint increments – informal). *Consider an Archimedean copula with generator φ and parameter τ . Given $(S(t_i), G(t_i))$ and the CIF increments $\Delta \text{CIF}_T, \Delta \text{CIF}_C$ over $(t_i, t_{i+1}]$, there exist sharp bounds $\underline{S}(t_{i+1}) \leq S(t_{i+1}) \leq \bar{S}(t_{i+1})$ and $\underline{G}(t_{i+1}) \leq G(t_{i+1}) \leq \bar{G}(t_{i+1})$, computable in closed form from φ and $(S(t_i), G(t_i))$. The bounds collapse to point estimates as $\max_i |t_{i+1} - t_i| \rightarrow 0$.*

The formal statement and proof are in Sec. D. After establishing bounds, we obtain point estimates via midpoint interpolation, $\hat{S}(t_{i+1}) = \frac{1}{2}(\underline{S}(t_{i+1}) + \bar{S}(t_{i+1}))$, and analogously for $\hat{G}(t)$, yielding a point-identified estimator of $S(t)$ as the grid becomes refined. Finally, after recovering $\hat{S}(t)$, which is the target quantity in the informative censoring setting, we may once again invoke Thm. 1 and compute the x -specific direct, indirect, and spurious effects of X on $S(t)$. This allows us to quantify causal fairness under informative censoring, through a sensitivity analysis based on the τ parameter.

Two Modeling Routes for Informative Censoring. The copula assumption in Eq. 13 may be imposed at two distinct levels of granularity, leading to two modeling approaches.

Route I (Conditional Copula Given Covariates). The first approach is to model the joint $P(T, C | X, Z, W)$ by an Archimedean copula with parameter τ . In this case, the dependence structure for (T, C) is specified conditionally on (X, Z, W) . However, in the IC setting, the survival $S(t | X, Z, W)$ is obtained recursively, with each step involving a complex non-linear map based on φ , making doubly-robust estimation difficult. We thus focus on model-based estimation for this route.

Route II (Population-Level Copula for Potential Outcomes). The second approach is to impose the copula assumption on the joint law of the *potential outcomes* (T, C) after marginalization over (Z, W) , that is, on quantities of the form

$$P(T_{x_y, W_{x_w}}, C_{x_y, W_{x_w}} | x_z). \quad (14)$$

In this case, the copula allows us to reconstruct population-level survival quantities from $\text{CIF}_T, \text{CIF}_C$, which can be estimated via a doubly-robust procedure. The sensitivity parameter τ is thus interpreted as governing dependence at the population level. The final challenge in this approach lies in the propagation of uncertainty over the CIF estimates into the uncertainty over the $P(T_{x_y, W_{x_w}} > t | x_z)$, which we discuss in Appx. D.1.

3 Case Study – Race Differentials in ICU

Finally, we showcase the usefulness of our methodology on a real-world study. Our task is to study racial disparities in outcome after admission to an intensive care unit (ICU). Disparities in post-ICU

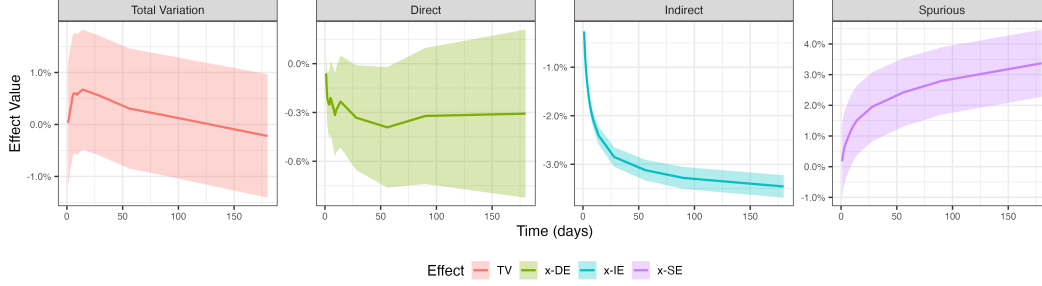


Figure 3: Case study results: survival curves, disparity metrics, and causal decompositions.

outcomes across race and ethnicity are known to exist [26, 34], although the topic has not been studied extensively in the literature. We make use of the data Adult Patient Database (APD) of the Australia and New Zealand Intensive Care Society (ANZICS) [41, 37], and the acknowledgement of contributing hospitals is given in Sec. E. The ANZICS APD receives submissions from 98% of ICUs in Australia. We differentiate four variable groups: indigenous status; sociodemographic variables (age, sex, postcode-based SES); ICU-relevant clinical variables, including the APACHE-III [21] predicted risk of death, ANZICS modified APACHE-III admission diagnosis (see full list of considered diagnoses), and indicator of whether admission was elective; and outcomes $\{T_1, T_2\}$, where T_1 is time to death after ICU admission as registered in the database or the National Death Index (NDI), while T_2 is the time to readmission to ICU as recorded in the database.

We now justify the causal structure. Indigenous status and sociodemographic variables may share common causes through historical and socioeconomic processes, but neither is a cause of the other, motivating the $X \leftrightarrow Z$ relationship and follows the modeling choice adopted in previous literature [26, 34]. Clinical variables are temporally downstream from both: for instance, indigenous status may influence illness severity through disparities in healthcare access, chronic disease burden, and preventive care. All variables may influence mortality and readmission. This justifies treating indigenous status as X , sociodemographics as confounders Z , clinical variables as mediators W , and survival times as the outcome.

We acknowledge two potential limitations regarding unmeasured confounding. First, genetic variation may act as a common cause of indigenous status and disease susceptibility, confounding the $X \rightarrow W$ relationship. Second, geographic remoteness may confound multiple relationships: it can independently influence indigenous status composition, clinical presentation at admission, and post-discharge outcomes (X , W , and T). Sensitivity analysis for such unmeasured confounding in mediation settings is an important direction for future work. We analyzed all admissions from 181 hospitals across Australia between January 1st 2023 to July 1st 2024, yielding a cohort of 249,958 patients, of whom 10,436 were Indigenous, $P(X = x_0) \approx 4.2\%$. In our setting, the censoring mechanism is related to the data extraction process (administrative reason), and hence the key assumption of non-informative censoring, implied by the conditional independence of T, C given X, Z, W is justified.

Non-Informative Censoring – Death Disparities. We first focus on differences in death rates, studying how survival disparities evolve over time. We consider non-zero values of direct, indirect, or spurious effects as evidence of disparities between groups. Due to administrative censoring, our setting falls under non-informative censoring (NIC) studied in Sec. 2. We begin by estimating the survival differences for x_0, x_1 populations over time, measured by the TV measure in Eq. 1, visualized in Fig. 3 (far left), which serves as a statistical baseline commonly used in the literature [35, 24]. As the plot shows, in the first 3 weeks after ICU admission, the survival is increasingly higher for the majority group x_1 , but after this the TV measure drops back down, with the point estimate negative at $T = 180$ days, meaning that minority patients have higher survival probability at that point in time. However, 95% confidence intervals (obtained assuming asymptotic normality of our cross-fitted doubly robust approach) include 0 after $T = 80$ days.

We then apply the temporal decomposition discussed in Sec. 2, breaking $P(T > t | X = x_1) - P(T > t | X = x_0)$ into contributions from the direct, indirect, and spurious pathways, for different values of t . The decomposition is shown in Fig. 3 (three facets to the right), and highlights interesting results that may be possibly overlooked by a classical statistical approach. First, we see that the direct

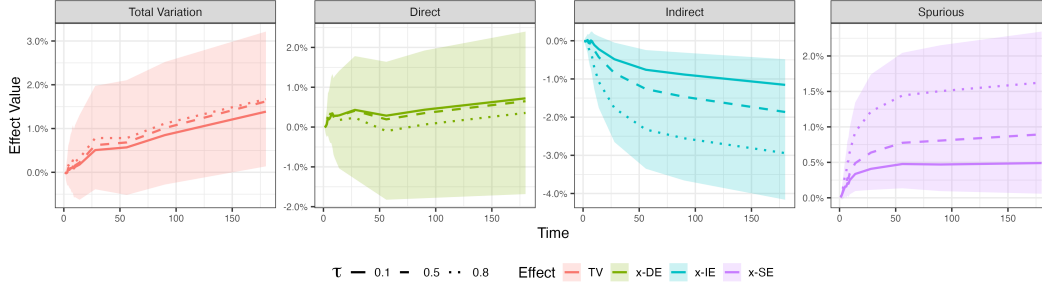


Figure 4: Case study results: survival curves, disparity metrics, and causal decompositions.

effect decreases up to $T = 50$ days after ICU admission, after which it stabilizes. The sign of this effect implies that minority patients experience *improved survival* along the direct path. Secondly, we see that the indirect effect decreases over time. The sign of the effect implies that minority patients have *reduced survival* along this causal pathway (due to higher burden of chronic and acute illness), which reaches almost 3% difference after $T = 50$ days, and continues to amplify up to $T = 180$ days. We remark these are rather large effects in a cohort with a marginal mortality rate of $< 10\%$. Thirdly, for the spurious effect, we see an increasing value up to $T = 180$ days. This implies that minority patients have improved survival along the spurious pathway, which can be related to lower overall age at admission, which naturally reduces the mortality rate. Taken together, the decomposition reveals that the near-zero TV measure masks substantial, opposing pathway-specific effects, uncovering a pattern that would be missed by standard statistical fairness analyses.

Informative Censoring – Readmission Disparities. In the second analysis, we focus on the readmission outcome as our primary target. Readmission is a relevant post-ICU outcome since it has a slightly different etiology than death, as it reflects downstream clinical stability, discharge decisions, and post-ICU recovery processes rather than acute physiological failure. Furthermore, readmission is also interesting as it has a direct implication on the burden of care placed on health systems. In this context, we wish to study the disparities in time-to-readmission $P(T_2 > t)$, in the hypothetical world where death does not act as a censoring outcome (clearly, in the real world, death prevents us from observing a possible need for readmission). Due to informativeness of death censoring for readmission, which has unobserved common causes with readmission (latent illness severity, unmeasured frailty, treatment limitations, post-discharge care quality), our setting falls under informative censoring (IC). We perform the sensitivity analysis from Sec. 2.2, and use Route II described therein for estimation of causal effects. Based on domain knowledge, we assume that event times T_1, T_2 are positively correlated ($\tau > 0$), as they share common causes that make both events more likely, including functional reserve, complications during ICU stay, and post-discharge care.

The results of the sensitivity analysis with $\tau \in \{0.1, 0.5, 0.8\}$ are shown in Fig. 4, where the ribbons indicate maximal and minimal 95% confidence intervals across τ values. The TV measure increases over time, meaning that burden of readmission is higher for minority patients. Along the direct effect, minority patients require more readmissions, opposite to the finding for the death outcome. However, the confidence bounds for these measures do not allow us to make definitive conclusions about effect sizes. Next, along the indirect effect, the burden of readmission is increased for the minority group, due to more complicated admission diagnoses and worse chronic health compared to the majority population. Finally, for the spurious effect, minority patients again have a lower burden of readmission, likely due to lower average age at time of ICU admission.

Limitations & Future Work. Our framework rests on the lack-of-confounding assumptions encoded in the SFM (Fig. 2a). While these assumptions are prevalent in the causal fairness literature [33, 46], they should not be taken for granted, but carefully justified on a case-by-case basis. Developing sensitivity analyses for causal decompositions in presence of unmeasured confounding is an important direction for future work. A further limitation is the reliance on the Archimedean copula assumption in the informative censoring setting (Sec. 2.2); while we treat τ as a sensitivity parameter, the choice of copula family itself is an additional modeling assumption that future work could relax. Finally, our formulation currently assumes time-invariant covariates; and our competing risks analysis does not isolate primary from competing hazard effects. We leave these extensions for future work.

References

- [1] O. Aalen. Nonparametric inference for a family of counting processes. *The Annals of Statistics*, pages 701–726, 1978.
- [2] J. Angwin, J. Larson, S. Mattu, and L. Kirchner. Machine bias: There’s software used across the country to predict future criminals. and it’s biased against blacks. *ProPublica*, 5 2016. URL <https://www.propublica.org/article/machine-bias-risk-assessments-in-criminal-sentencing>.
- [3] H. Bang and J. M. Robins. Doubly robust estimation in missing data and causal inference models. *Biometrics*, 61(4):962–973, 2005.
- [4] F. D. Blau and L. M. Kahn. The gender earnings gap: learning from international comparisons. *The American Economic Review*, 82(2):533–538, 1992.
- [5] F. D. Blau and L. M. Kahn. The gender wage gap: Extent, trends, and explanations. *Journal of economic literature*, 55(3):789–865, 2017.
- [6] R. Braekers and N. Veraverbeke. A copula-graphic estimator for the conditional survival function under dependent censoring. *Canadian Journal of Statistics*, 33(3):429–447, 2005.
- [7] T. Brennan, W. Dieterich, and B. Ehret. Evaluating the predictive validity of the compas risk and needs assessment system. *Criminal Justice and Behavior*, 36(1):21–40, 2009.
- [8] J. Buolamwini and T. Gebru. Gender shades: Intersectional accuracy disparities in commercial gender classification. In S. A. Friedler and C. Wilson, editors, *Proceedings of the 1st Conference on Fairness, Accountability and Transparency*, volume 81 of *Proceedings of Machine Learning Research*, pages 77–91, NY, USA, 2018.
- [9] T. Chen and C. Guestrin. Xgboost: A scalable tree boosting system. In *Proceedings of the 22nd acm sigkdd international conference on knowledge discovery and data mining*, pages 785–794, 2016.
- [10] V. Chernozhukov, D. Chetverikov, M. Demirer, E. Duflo, C. Hansen, W. Newey, and J. Robins. Double/debiased machine learning for treatment and structural parameters, 2018.
- [11] S. Chiappa. Path-specific counterfactual fairness. In *Proceedings of the AAAI Conference on Artificial Intelligence*, volume 33, pages 7801–7808, 2019.
- [12] E. Creager, D. Madras, T. Pitassi, and R. Zemel. Causal modeling for fairness in dynamical systems. In *International conference on machine learning*, pages 2185–2195. PMLR, 2020.
- [13] A. Datta, M. C. Tschantz, and A. Datta. Automated experiments on ad privacy settings: A tale of opacity, choice, and discrimination. *Proceedings on Privacy Enhancing Technologies*, 2015 (1):92–112, Apr. 2015. doi: 10.1515/popets-2015-0007.
- [14] J. P. Fine and R. J. Gray. A proportional hazards model for the subdistribution of a competing risk. *Journal of the American statistical association*, 94(446):496–509, 1999.
- [15] I. O. Gallegos, R. A. Rossi, J. Barrow, M. M. Tanjim, S. Kim, F. Derroncourt, T. Yu, R. Zhang, and N. K. Ahmed. Bias and fairness in large language models: A survey. *Computational Linguistics*, 50(3):1097–1179, 2024.
- [16] S. Hu and G. H. Chen. Fairness in survival analysis with distributionally robust optimization. *Journal of machine learning research*, 25(246):1–85, 2024.
- [17] H. Ishwaran, U. B. Kogalur, E. H. Blackstone, and M. S. Lauer. Random survival forests. *The Annals of Applied Statistics*, 2(3):841–860, Sept. 2008. doi: 10.1214/08-AOAS169.
- [18] E. L. Kaplan and P. Meier. Nonparametric estimation from incomplete observations. *Journal of the American statistical association*, 53(282):457–481, 1958.
- [19] A. E. Khandani, A. J. Kim, and A. W. Lo. Consumer credit-risk models via machine-learning algorithms. *Journal of Banking & Finance*, 34(11):2767–2787, 2010.

- [20] J. P. Klein and M. L. Moeschberger. *Survival Analysis*. Statistics for Biology and Health. Springer, New York, NY, 1 edition, September 1999.
- [21] W. A. Knaus, D. P. Wagner, E. A. Draper, J. E. Zimmerman, M. Bergner, P. G. Bastos, C. A. Sirio, D. J. Murphy, T. Lotring, A. Damiano, et al. The apache iii prognostic system: risk prediction of hospital mortality for critically iii hospitalized adults. *Chest*, 100(6):1619–1636, 1991.
- [22] M. J. Kusner, J. Loftus, C. Russell, and R. Silva. Counterfactual fairness. *Advances in neural information processing systems*, 30, 2017.
- [23] T. Lange and J. V. Hansen. Direct and indirect effects in a survival context. *Epidemiology*, 22(4):575–581, 2011.
- [24] M. Liu, Y. Ning, H. Wang, C. Hong, M. Engelhard, D. S. Bitterman, W. G. La Cava, and N. Liu. Equitable survival prediction: A fairness-aware survival modeling (fasm) approach. *arXiv preprint arXiv:2510.20629*, 2025.
- [25] J. F. Mahoney and J. M. Mohen. Method and system for loan origination and underwriting, Oct. 23 2007. US Patent 7,287,008.
- [26] S. K. McGowan, K. A. Sarigiannis, S. C. Fox, M. A. Gottlieb, and E. Chen. Racial disparities in icu outcomes: a systematic review. *Critical care medicine*, 50(1):1–20, 2022.
- [27] R. Nabi, D. Malinsky, and I. Shpitser. Learning optimal fair policies. In *International conference on machine learning*, pages 4674–4682. PMLR, 2019.
- [28] W. Nelson. Theory and applications of hazard plotting for censored failure data. *Technometrics*, 14(4):945–966, 1972.
- [29] D. Pager. The mark of a criminal record. *American journal of sociology*, 108(5):937–975, 2003.
- [30] J. Pearl. *Causality: Models, Reasoning, and Inference*. Cambridge University Press, New York, 2000. 2nd edition, 2009.
- [31] D. Pessach and E. Shmueli. A review on fairness in machine learning. *ACM Computing Surveys (CSUR)*, 55(3):1–44, 2022.
- [32] T.-H. Pham, J. Chen, S. Lee, Y. Wang, S. Moroi, X. Zhang, and P. Zhang. The boundaries of fair ai in medical image prognosis: A causal perspective. *arXiv preprint arXiv:2510.08840*, 2025.
- [33] D. Plečko and E. Bareinboim. Causal fairness analysis: A causal toolkit for fair machine learning. *Foundations and Trends® in Machine Learning*, 17(3):304–589, 2024.
- [34] D. Plecko, P. Secombe, A. Clarke, A. Fiske, S. Toby, D. Duff, D. Pilcher, L. A. Celi, R. Bellomo, and E. Bareinboim. An algorithmic approach for causal health equity: A look at race differentials in intensive care unit (icu) outcomes. *arXiv preprint arXiv:2501.05197*, 2025.
- [35] M. M. Rahman and S. Purushotham. Fair and interpretable models for survival analysis. In *Proceedings of the 28th ACM SIGKDD Conference on Knowledge Discovery and Data Mining*, pages 1452–1462, 2022.
- [36] P. Royston and M. K. Parmar. Restricted mean survival time: an alternative to the hazard ratio for the design and analysis of randomized trials with a time-to-event outcome. *BMC medical research methodology*, 13(1):152, 2013.
- [37] P. Secombe, J. Millar, E. Litton, S. Chavan, T. Hensman, G. K. Hart, A. Slater, R. Herkes, S. Huckson, and D. V. Pilcher. Thirty years of anzics core: a clinical quality success story. *Critical Care and Resuscitation*, 25(1):43–46, 2023.
- [38] M. Y. Shaheen. Applications of artificial intelligence (ai) in healthcare: A review. *ScienceOpen Preprints*, 2021.
- [39] I. Shpitser and J. Pearl. What counterfactuals can be tested. In *Proceedings of the Twenty-third Conference on Uncertainty in Artificial Intelligence*, page 352–359, 2007.

- [40] R. Sonabend, F. Pfisterer, A. Mishler, M. Schauer, L. Burk, S. Mukherjee, and S. Vollmer. Flexible group fairness metrics for survival analysis. *arXiv preprint arXiv:2206.03256*, 2022.
- [41] P. J. Stow, G. K. Hart, T. Higlett, C. George, R. Herkes, D. McWilliam, R. Bellomo, A. D. M. Committee, et al. Development and implementation of a high-quality clinical database: the australian and new zealand intensive care society adult patient database. *Journal of critical care*, 21(2):133–141, 2006.
- [42] L. Sweeney. Discrimination in online ad delivery. Technical Report 2208240, SSRN, Jan. 28 2013. URL <http://dx.doi.org/10.2139/ssrn.2208240>.
- [43] L. T. Sweeney and C. Haney. The influence of race on sentencing: A meta-analytic review of experimental studies. *Behavioral Sciences & the Law*, 10(2):179–195, 1992.
- [44] T. J. VanderWeele. Causal mediation analysis with survival data. *Epidemiology*, 22(4):582–585, 2011.
- [45] T. Xie and Y. Ge. Fairness in survival analysis: A novel conditional mutual information augmentation approach. *arXiv preprint arXiv:2502.02567*, 2025.
- [46] J. Zhang and E. Bareinboim. Fairness in decision-making—the causal explanation formula. In *Proceedings of the AAAI Conference on Artificial Intelligence*, volume 32, 2018.

Technical Appendices for *Causal Fairness for Survival Analysis*

The source code for reproducing all the experiments can be found in our anonymized code repository <https://anonymous.4open.science/r/cfa-survival-B880>. All experiments were performed on a MacBook Pro, with the M3 Pro chip and 36 GB RAM on macOS 26.2 (Tahoe). All experiments can be run with less than 24 hours of compute on the above-described machine or equivalent.

A Proofs

Thm. 1 Proof: Let \mathcal{M} be an SCM compatible with the SFM in Fig. 2d, and let f_T be the structural mechanism of T , taking X, Z, W as inputs together with the noise variables U_T, U_C . The conditional distribution $P(T | X = x, Z = z, W = w)$ is determined by f_T and the distribution of the noise variables, and depends on X, Z, W only through their realized values x, z, w . Therefore, the random variable $\Phi \triangleq \phi(P(T | X, Z, W))$ has the structural mechanism

$$f_\Phi(x, z, w) = \phi(P(T | X = x, Z = z, W = w)), \quad (15)$$

which is a deterministic function of X, Z, W and does not depend on any of the noise variables U . Consequently, Φ can be added to the causal diagram as in Fig. 2b, completing the proof. \square

Prop. 1 Proof: We demonstrate that the potential outcome $\mathbb{E}[\Phi_{x_y, W_{x_w}}(t) | X = x_z]$ is identifiable under the Standard Fairness Model. For this purpose, we make use of the counterfactual graph [39] in Fig. 5. We expand $\mathbb{E}[\Phi_{x_y, W_{x_w}}(t) | x_z]$ as follows:

$$= \sum_w \mathbb{E}[\Phi_{x_y, w}(t) \mathbb{1}(W_{x_w} = w) | x_z] \quad (\text{Counterfactual Un-nesting}) \quad (16)$$

$$= \sum_{z, w} \mathbb{E}[\Phi_{x_y, w}(t) \mathbb{1}(W_{x_w} = w) | z, x_z] P(z | x_z) \quad (\text{Law of Total Probability}) \quad (17)$$

$$= \sum_{z, w} \mathbb{E}[\Phi_{x_y, w}(t) | z, x_z] P(W_{x_w} = w | z, x_z) P(z | x_z) \quad (\Phi_{x_y, w} \perp\!\!\!\perp W_{x_w} | Z, X) \quad (18)$$

$$= \sum_{z, w} \mathbb{E}[\Phi_{x_y, w}(t) | z, x_z] P(W_{x_w} = w | z, x_w) P(z | x_z) \quad (W_{x_w} \perp\!\!\!\perp X | Z) \quad (19)$$

$$= \sum_{z, w} \mathbb{E}[\Phi_{x_y, w}(t) | z, x_z] P(W = w | z, x_w) P(z | x_z) \quad (\text{Consistency}) \quad (20)$$

$$= \sum_{z, w} \mathbb{E}[\Phi_{x_y, w}(t) | z, w, x_z] P(W = w | z, x_w) P(z | x_z) \quad (\Phi_{x_y, w} \perp\!\!\!\perp W | Z, X) \quad (21)$$

$$= \sum_{z, w} \mathbb{E}[\Phi_{x_y, w}(t) | z, w, x_y] P(W = w | z, x_w) P(z | x_z) \quad (\Phi_{x_y, w} \perp\!\!\!\perp X | Z, W) \quad (22)$$

$$= \sum_{z, w} \mathbb{E}[\Phi(t) | z, w, x_y] P(W = w | z, x_w) P(z | x_z) \quad (\text{Consistency}), \quad (23)$$

which completes the proof. \square

Prop. 2 Proof: We focus on the quantity $\mathbb{E}[\Phi_{x_y, W_{x_w}}(t) | x_z]$. Suppose that we have:

$$f(x_y, z, w) \xrightarrow{P} \mathbb{E}[\Phi(t) | x_y, z, w] \quad \forall z, w \quad (24)$$

$$\hat{P}(x_w | w, z) \xrightarrow{P} P(x_w | w, z) \quad \forall z, w \quad (25)$$

$$\hat{P}(x_w | z) \xrightarrow{P} P(x_w | z) \quad \forall z \quad (26)$$

$$\hat{P}(x_z | z) \xrightarrow{P} P(x_z | z) \quad \forall z \quad (27)$$

$$\hat{P}(z, w) \xrightarrow{P} P(z, w) \quad \forall w, z \quad (28)$$

$$\hat{P}(x_z) \xrightarrow{P} P(x_z) \quad (29)$$

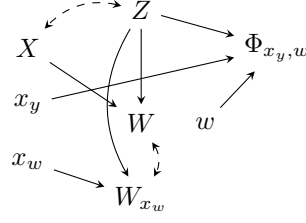


Figure 5: Counterfactual graph of the SFM used in the proof of Prop. 1.

where f and the $\hat{P}(\cdot | \cdot)$ terms are estimators, and $\hat{P}(z, w)$, $\hat{P}(x_z)$ are the empirical distributions:

$$\hat{P}(z, w) = \frac{1}{n} \sum_{i=1}^n \mathbb{1}(Z_i = z, W_i = w) \quad (30)$$

$$\hat{P}(x_z) = \frac{1}{n} \sum_{i=1}^n \mathbb{1}(X_i = x_z). \quad (31)$$

Applying Bayes' rule to the identification expression in Eq. 23, we re-write it as:

$$\sum_{z, w} \mathbb{E}[\Phi(t) | z, w, x_y] P(z, w) \frac{P(x_w | w, z)}{P(x_w | z)} \frac{P(x_z | z)}{P(x_z)}. \quad (32)$$

By a coupling of quantities in Eqs. 24-29 to a joint probability space and an application of the continuous mapping theorem we obtain that

$$\sum_{z, w} f(x_y, z, w) \hat{P}(z, w) \frac{\hat{P}(x_w | w, z)}{\hat{P}(x_w | z)} \frac{\hat{P}(x_z | z)}{\hat{P}(x_z)} \quad (33)$$

$$\xrightarrow{P} \sum_{z, w} \mathbb{E}[\Phi(t) | z, w, x_y] P(z, w) \frac{P(x_w | w, z)}{P(x_w | z)} \frac{P(x_z | z)}{P(x_z)}. \quad (34)$$

Finally, note that we have

$$\sum_{z, w} f(x_y, z, w) \hat{P}(z, w) \frac{\hat{P}(x_w | w, z)}{\hat{P}(x_w | z)} \frac{\hat{P}(x_z | z)}{\hat{P}(x_z)} \quad (35)$$

$$= \sum_{z, w} f(x_y, z, w) \left(\sum_{i=1}^n \frac{\mathbb{1}(Z_i = z, W_i = w)}{n} \right) \frac{\hat{P}(x_w | w, z)}{\hat{P}(x_w | z)} \frac{\hat{P}(x_z | z)}{\hat{P}(x_z)} \quad (36)$$

$$= \frac{1}{n} \sum_{i=1}^n f(x_y, z_i, w_i) \frac{\hat{P}(x_w | w_i, z_i)}{\hat{P}(x_w | z_i)} \frac{\hat{P}(x_z | z_i)}{\hat{P}(x_z)}, \quad (37)$$

completing the proof of the proposition. \square

The proof of Thm. 2 is given in Sec. C, while the proof of Thm. 3 is given in Sec. D.

B Alternative Scales for Quantifying Survival Disparities

In this appendix, we discuss alternative scales for quantifying survival disparities across demographic groups, beyond the survival difference metric used in the main text (see Eq. 1). The alternative metrics that may be of interest include restricted mean survival time (RMST) differences [36] and (cumulative) hazard ratios [20]. Importantly, all such metrics can be accommodated within the causal framework developed in this paper. Formally, we may be interested in a metric $d(P(T | X = x_1), P(T | X = x_0))$, where $P(T | X = x)$ denotes the survival distribution for group $X = x$. The possible quantities of interest include:

(i) *Survival differences* (used in Sec. 2)

$$P(T > t | X = x_1) - P(T > t | X = x_0), \quad t \in [0, \infty), \quad (38)$$

(ii) *Restricted mean survival time (RMST) differences*

$$\mathbb{E}[\min\{T, t\} | X = x_1] - \mathbb{E}[\min\{T, t\} | X = x_0], \quad t \in [0, \infty), \quad (39)$$

(iii) *(Cumulative) hazard ratios*

$$\frac{\mathbb{E}[\eta(t | X, Z, W) | X = x_1]}{\mathbb{E}[\eta(t | X, Z, W) | X = x_0]}, \quad t \in [0, \infty), \quad (40)$$

where $\eta(t | X, Z, W)$ denotes the (cumulative) hazard function.

These metrics provide different scales on which time-evolving disparities between groups may be quantified (depending on the subject question of interest). Regardless of the chosen metric, our objective is to decompose each such disparity measure into contributions arising from the direct path $X \rightarrow T$, the indirect path $X \rightarrow W \rightarrow T$, and the spurious path $X \leftrightarrow Z \rightarrow T$.

Reduction to a Deterministic Outcome. As described in Sec. 2, the key observation enabling a unified treatment of the above disparity measures is that each can be written as a functional of the conditional distribution $P(T | X, Z, W)$. Specifically, let ϕ be a functional mapping $P(T | X, Z, W)$ to \mathbb{R} , and define the random variable

$$\Phi \triangleq \phi(P(T | X, Z, W)). \quad (41)$$

Here, Φ is a deterministic function of (X, Z, W) , while ϕ operates on the conditional survival distribution. With this notation, each metric above can be written either on a difference scale,

$$\mathbb{E}[\Phi | X = x_1] - \mathbb{E}[\Phi | X = x_0], \quad (42)$$

or on a ratio scale,

$$\frac{\mathbb{E}[\Phi | X = x_1]}{\mathbb{E}[\Phi | X = x_0]}. \quad (43)$$

For example, taking $\Phi = P(T > t | X, Z, W)$ in Eq. 42 yields the survival difference metric in (i), while taking $\Phi = \eta(t | X, Z, W)$ in Eq. 43 yields the cumulative hazard ratio metric in (iii). As described in Thm. 1, since Φ is a deterministic function of (X, Z, W) , it does not depend on any exogenous noise variables. Consequently, Φ may be added as a node to the causal graph implied by the Standard Fairness Model (SFM), inheriting the same causal structure as any other deterministic transformation of (X, Z, W) . This observation allows us to define direct, indirect, and spurious effects of X on Φ , and the associated TV decomposition as in Eq. 4. The RMST metric in (ii) can be analyzed using the same decomposition. Ratio metrics as in (iii), however, require a different approach. Here we provide the formal result that allows us to decompose statistical differences on the ratio scale into their causal contributions along pathways:

Proposition 3 (*x-specific Decomposition for Ratio Scales*). *Let Φ denote a random variable. The x-specific direct, indirect, and spurious ratio-scale effects of X on Φ are defined as*

$$x\text{-DR}_{x_0, x_1}(\Phi | x) = \frac{\mathbb{E}[\Phi_{x_1, W_{x_0}} | X = x]}{\mathbb{E}[\Phi_{x_0, W_{x_0}} | X = x]}, \quad (44)$$

$$x\text{-IR}_{x_1, x_0}(\Phi | x) = \frac{\mathbb{E}[\Phi_{x_1, W_{x_0}} | X = x]}{\mathbb{E}[\Phi_{x_1} | X = x]}, \quad (45)$$

$$x\text{-SR}_{x_1, x_0}(\Phi) = \frac{\mathbb{E}[\Phi_{x_1} | X = x_0]}{\mathbb{E}[\Phi_{x_1} | X = x_1]}. \quad (46)$$

Using these measures, the total variation ratio $\frac{\mathbb{E}[\Phi | x_1]}{\mathbb{E}[\Phi | x_0]}$ can be decomposed as:

$$\frac{\mathbb{E}[\Phi | x_1]}{\mathbb{E}[\Phi | x_0]} = x\text{-DR}_{x_0, x_1}(\Phi | x_0) \times [x\text{-IR}_{x_1, x_0}(\Phi | x_0)]^{-1} \times [x\text{-SR}_{x_1, x_0}(\Phi)]^{-1}. \quad (47)$$

Prop. 3 can be seen as an analogue of the result in Eq. 4 that is useful for metrics where ratios are more natural than differences, such as hazard ratios or cumulative hazard ratios [20].

C Doubly Robust Estimation

In this appendix, we describe the construction of influence functions for the causal estimands used in Sec. 2. We first focus on the potential outcomes of the survival curve $S(t | X, Z, W)$. For a fixed $t \geq 0$, our target parameter $\psi(t)$ is the potential outcome $\mathbb{E}[S_{x_y, W_{x_w}}(t) | X = x_z]$, where $S_{x_y, W_{x_w}}(t) = P(T_{x_y, W_{x_w}} > t)$. Under the Standard Fairness Model (Fig. 2a) with non-informative censoring $T \perp\!\!\!\perp C | X, Z, W$, Prop. 1 shows that the identification expression for $\psi(t)$ is given by

$$\psi(t) = \sum_{z, w} S(t | x_y, z, w) P(w | x_w, z) P(z | x_z). \quad (48)$$

As before, we denote the observed data quantities $M = \min\{T, C\}$ and $\delta = \mathbb{1}(T \leq C)$. Due to independence, note that

$$S(t | X, Z, W) = \mathbb{E} \left[\frac{\mathbb{1}(M > t)}{G(t | X, Z, W)} \middle| X, Z, W \right], \quad (49)$$

where $G(t | X, Z, W) = P(C > t | X, Z, W)$ is the censoring survival function.

Influence Function Derivation. We then compute the influence function of the identification expression in Eq. 48, which can be obtained as:

$$\mathbb{IF}(\psi(t)) = \sum_{z, w} \underbrace{\mathbb{IF}(S(t | x_y, z, w)) P(w | x_w, z) P(z | x_z)}_{T_1} \quad (50)$$

$$+ \underbrace{S(t | x_y, z, w) \mathbb{IF}(P(w | x_w, z)) P(z | x_z)}_{T_2}$$

$$+ \underbrace{S(t | x_y, z, w) P(w | x_w, z) \mathbb{IF}(P(z | x_z))}_{T_3}, \quad (51)$$

using the fact that $\mathbb{IF}(AB) = \mathbb{IF}(A) \cdot B + A \cdot \mathbb{IF}(B)$. Let $\xi_1(t)$ and $\xi_2(t)$ denote the augmentation terms defined in Thm. 2. The individual influence functions for each of the appearing terms can be obtained as:

$$\mathbb{IF}(S(t | x_y, z, w)) = \frac{\mathbb{1}(X = x_y, Z = z, W = w)}{P(x_y, z, w)} \quad (52)$$

$$\cdot \left[\frac{\mathbb{1}(M > t)}{G(t | X, Z, W)} + \xi_1(t) - \xi_2(t) - S(t | x_y, z, w) \right], \quad (53)$$

$$\mathbb{IF}(P(w | x_w, z)) = \frac{\mathbb{1}(X = x_w, Z = z)}{P(x_w, z)} [\mathbb{1}(W = w) - P(w | x_w, z)], \quad (54)$$

$$\mathbb{IF}(P(z | x_z)) = \frac{\mathbb{1}(X = x_z)}{P(x_z)} [\mathbb{1}(Z = z) - P(z | x_z)]. \quad (55)$$

Substituting into T_1 gives

$$\frac{\mathbb{1}(X = x_y)}{P(x_z)} \frac{P(x_z | Z)}{P(x_w | Z)} \frac{P(x_w | Z, W)}{P(x_y | Z, W)} \left[\frac{\mathbb{1}(M > t)}{G(t | X, Z, W)} + \xi_1(t) - \xi_2(t) - S(t | X, Z, W) \right], \quad (56)$$

whereas substituting into T_2, T_3 yields

$$T_2 = \frac{\mathbb{1}(X = x_w)}{P(x_z)} \frac{P(x_z | Z)}{P(x_w | Z)} [S(t | x_y, Z, W) - \mathbb{E}[S(t | x_y, Z, W) | x_w, Z]], \quad (57)$$

$$T_3 = \frac{\mathbb{1}(X = x_z)}{P(x_z)} \mathbb{E}[S(t | x_y, Z, W) | x_w, Z] - \frac{\mathbb{1}(X = x_z)}{P(x_z)} \psi(t). \quad (58)$$

Combining the terms yields the influence function stated in Thm. 2.

Double Robustness. Let S, G denote the true survival and censoring functions, and let \hat{S}, \hat{G} denote their estimates. Let the true censoring density be $f_C(u) = -G'(u)$ and the estimated censoring hazard be $\hat{h}_C(u) = \frac{-\hat{G}'(u)}{\hat{G}(u)}$. Because $T \perp\!\!\!\perp C \mid X, Z, W$, the joint density of (T, C) factors as $f_T(t)f_C(c)$ conditionally. For brevity, we suppress covariate conditioning. The term in the bracket in Eq. 56 is $D(t) = \frac{\mathbb{1}(M > t)}{\hat{G}(t)} + \xi_1(t) - \xi_2(t) - S(t)$, where:

$$\xi_1(t) = \hat{S}(t) \frac{\mathbb{1}(M \leq t, \delta = 0)}{\hat{S}(M)\hat{G}(M)}, \quad \xi_2(t) = \hat{S}(t) \int_0^t \frac{\mathbb{1}(M \geq u)}{\hat{S}(u)\hat{G}(u)} \hat{h}_C(u) du. \quad (59)$$

We want to show consistency $\mathbb{E}[D(t)] = 0$ under misspecification of either S or G .

Case 1 ($\hat{G} = G, \hat{S}$ is arbitrary). Because the estimated censoring model matches the true distribution, we have $\hat{G}(u) = G(u)$ and the estimated hazard is the true hazard, $\hat{h}_C(u) = \frac{-G'(u)}{G(u)}$. The expected value of the IPCW term is simply $\mathbb{E}[\frac{\mathbb{1}(M > t)}{G(t)}] = \frac{P(T > t, C > t)}{G(t)} = \frac{S(t)G(t)}{G(t)} = S(t)$. The censoring event $\delta = 0$ in term $\xi_1(t)$ triggers only when $C \leq t$ and $T > C$, so the term can be re-written as an integral:

$$\begin{aligned} \mathbb{E}[\xi_1(t)] &= \hat{S}(t) \int_0^t \int_c^\infty \frac{1}{\hat{S}(c)G(c)} f_T(u) f_C(c) du dc \\ &= \hat{S}(t) \int_0^t \frac{P(T > c)}{\hat{S}(c)G(c)} f_C(c) dc = \hat{S}(t) \int_0^t \frac{S(c)}{\hat{S}(c)G(c)} (-G'(c)) dc. \end{aligned} \quad (60)$$

For the term $\xi_2(t)$, we have $\mathbb{E}[\mathbb{1}(M \geq u)] = P(T \geq u, C \geq u) = S(u)G(u)$. Thus:

$$\mathbb{E}[\xi_2(t)] = \hat{S}(t) \int_0^t \frac{\mathbb{E}[\mathbb{1}(M \geq u)]}{\hat{S}(u)G(u)} \left(\frac{-G'(u)}{G(u)} \right) du = \hat{S}(t) \int_0^t \frac{S(u)}{\hat{S}(u)G(u)} (-G'(u)) du. \quad (61)$$

Comparing Eq. 60 and Eq. 61, we see $\mathbb{E}[\xi_1(t)] = \mathbb{E}[\xi_2(t)]$, so their difference strictly evaluates to zero. Hence, $\mathbb{E}[D(t)] = \mathbb{E}[\frac{\mathbb{1}(M > t)}{G(t)}] - S(t) = 0$.

Case 2 ($\hat{S} = S, \hat{G}$ is arbitrary). Here, the IPCW exhibits a bias, namely $\mathbb{E}[\frac{\mathbb{1}(M > t)}{\hat{G}(t)}] = \frac{S(t)G(t)}{\hat{G}(t)} \neq S(t)$. Similarly to Eqs. (60) and (61), we evaluate the expected augmentation terms, this time under the correct S but misspecified \hat{G} :

$$\mathbb{E}[\xi_1(t)] = S(t) \int_0^t \frac{-G'(c)}{\hat{G}(c)} dc, \quad (62)$$

$$\mathbb{E}[\xi_2(t)] = S(t) \int_0^t \frac{S(u)G(u)}{S(u)\hat{G}(u)} \left(\frac{-\hat{G}'(u)}{\hat{G}(u)} \right) du = S(t) \int_0^t \frac{-G(u)\hat{G}'(u)}{\hat{G}(u)^2} du. \quad (63)$$

Subtracting Eq. 63 from Eq. 62 results in an integral of a differentiated quotient $\frac{-G(u)}{\hat{G}(u)}$:

$$\begin{aligned} \mathbb{E}[\xi_1(t) - \xi_2(t)] &= S(t) \int_0^t \left(\frac{-G'(u)\hat{G}(u) + G(u)\hat{G}'(u)}{\hat{G}(u)^2} \right) du = S(t) \int_0^t \frac{d}{du} \left(\frac{-G(u)}{\hat{G}(u)} \right) du \\ &= S(t) \left[\frac{-G(t)}{\hat{G}(t)} - \frac{-G(0)}{\hat{G}(0)} \right] = S(t) - \frac{S(t)G(t)}{\hat{G}(t)}, \end{aligned} \quad (64)$$

using $G(0) = \hat{G}(0) = 1$. Finally, plugging this into $\mathbb{E}[D(t)] = \frac{S(t)G(t)}{\hat{G}(t)} + S(t) - \frac{S(t)G(t)}{\hat{G}(t)} - S(t) = 0$ gives the desired result for the second case.

C.1 Influence Function for the CIF

Our next goal is to derive the influence function for the cumulative incidence functions used in Sec. 2.1. In this case, for cause k , the survival function $S(t \mid X, Z, W)$ is replaced by the cumulative incidence

function $\text{CIF}_k(t | X, Z, W) = P(T_k \leq t, \delta = k | X, Z, W)$. The identification expression for the CIF potential outcome $\mathbb{E}[(\text{CIF}_k)_{x_y, W_{x_w}} | X = x_z]$ is given by

$$\psi(t) = \sum_{z, w} \text{CIF}_k(t | x_y, z, w) P(w | x_w, z) P(z | x_z). \quad (65)$$

To obtain the influence function for the CIF identification expression, we proceed very similarly as in the survival function case. Under $C \perp\!\!\!\perp (T_1, \dots, T_K) | X, Z, W$ (see Fig. 2c), we have that

$$\text{CIF}_k(t | X, Z, W) = \mathbb{E} \left[\frac{\mathbb{1}(M \leq t, \delta = k)}{G(M | X, Z, W)} \middle| X, Z, W \right]. \quad (66)$$

Therefore, compared to terms T_1, T_2, T_3 in Eqs. 56-58, the term $\frac{\mathbb{1}(M > t)}{G(t | X, Z, W)}$ is replaced by $\frac{\mathbb{1}(M \leq t, \delta = k)}{G(M | X, Z, W)}$, and $S(t)$ is replaced by $\text{CIF}_k(t)$ throughout, yielding the following influence function

$$\mathbb{IF}(\psi(t)) = \frac{\mathbb{1}(X = x_y)}{P(x_z)} \frac{P(x_z | Z)}{P(x_w | Z)} \frac{P(x_w | Z, W)}{P(x_y | Z, W)} \left[\frac{\mathbb{1}(M \leq t, \delta = k)}{G(M | X, Z, W)} - \text{CIF}_k(t | X, Z, W) \right] \quad (67)$$

$$+ \frac{\mathbb{1}(X = x_w)}{P(x_z)} \frac{P(x_z | Z)}{P(x_w | Z)} [\text{CIF}_k(t | x_y, Z, W) - \mathbb{E}[\text{CIF}_k(t | x_y, Z, W) | X = x_w, Z]] \quad (68)$$

$$+ \frac{\mathbb{1}(X = x_z)}{P(x_z)} \mathbb{E}[\text{CIF}_k(t | x_y, Z, W) | X = x_w, Z] - \frac{\mathbb{1}(X = x_z)}{P(x_z)} \psi(t). \quad (69)$$

Doubly Robust Estimation and Cross-Fitting. When performing estimation we use cross-fitting.

Data is split into K folds $\mathcal{D}_1, \dots, \mathcal{D}_K$. Let $\widehat{\text{IF}}_{\psi(t)}^{-(k)}(V_i)$ denote the influence function evaluated for the observed sample V_i using nuisance estimators fitted on the complement of fold k , denoted as \mathcal{D}_{-k} . Using one-step debiasing, the cross-fitted estimator for $\psi(t)$ is given by

$$\hat{\psi}(t) = \frac{1}{n} \sum_{k=1}^K \sum_{i \in \mathcal{D}_k} \left\{ \frac{\mathbb{1}(X_i = x_z)}{\widehat{P}^{-(k)}(x_z)} \hat{\psi}^{-(k)}(t) + \widehat{\text{IF}}_{\psi(t)}^{-(k)}(V_i) \right\}, \quad (70)$$

where $\hat{\psi}^{-(k)}$ is the standard fold-specific plug-in estimator, given by

$$\hat{\psi}^{-(k)}(t) = \frac{1}{|\mathcal{D}_{-k}|} \sum_{i \in \mathcal{D}_{-k}} \hat{f}^{-(k)}(t | x_y, Z_i, W_i) \frac{\widehat{P}^{-(k)}(X_i = x_w | Z_i, W_i)}{\widehat{P}^{-(k)}(X_i = x_w | Z_i)} \frac{\widehat{P}^{-(k)}(X_i = x_z | Z_i)}{\widehat{P}^{-(k)}(X_i = x_z)}, \quad (71)$$

where \hat{f} is either the estimate of the survival function S or the CIF_k as appropriate. The estimator is doubly robust: it is consistent if either $S(t | X, Z, W)$ and $G(t | X, Z, W)$ are consistently estimated, or the propensity scores $P(X | Z)$ and $P(X | Z, W)$ are consistently estimated. All nuisance functions are estimated using flexible machine learning methods, with cross-fitting used to control overfitting bias, known as double machine learning [10]. For estimating causal effects, differences of estimators of the form $\hat{\psi}(t)$ are used, and we obtain confidence intervals assuming asymptotic normality, with the asymptotic variance obtained from the variance of the estimated influence function [10].

D Copula-Graphic Estimator

In this appendix, we summarize the copula-graphic estimator (CGE) used in Sec. 2.2 [6]. We consider a single event of interest with time-to-event T and a censoring time C informative for T . Following the notation in Sec. 2, we have that

$$S(t) = P(T > t), \quad G(t) = P(C > t), \quad (72)$$

$$S_{\text{all}}(t) = P(T > t, C > t), \quad H(t, c) = P(T > t, C > c). \quad (73)$$

Further, we write $\text{CIF}_T(t) = P(T \leq t, \delta = 1)$ and $\text{CIF}_C(t) = P(C \leq t, \delta = 0)$ for the CIFs of the event and censoring, respectively. Note that $S_{\text{all}}(t) = 1 - \text{CIF}_T(t) - \text{CIF}_C(t)$ by definition. As described in Sec. 2.2, we assume an Archimedean copula with generator φ (parameterized by Kendall's τ correlation coefficient) linking the joint survival and marginals as $H(t, c) = C_\tau(S(t), G(c))$, implying the following relation:

$$\varphi(S_{\text{all}}(t)) = \varphi(S(t)) + \varphi(G(t)). \quad (74)$$

Here, we first describe the copula-graphic estimator in the standard setting.

Classical copula-graphic recursion. Let $0 = t_0 < t_1 < \dots < t_m$ be a grid of time points and define the CIF increments

$$\Delta\text{CIF}_{i,T} = \text{CIF}_T(t_i) - \text{CIF}_T(t_{i-1}), \quad \Delta\text{CIF}_{i,C} = \text{CIF}_C(t_i) - \text{CIF}_C(t_{i-1}), \quad (75)$$

and the corresponding decrease of the joint survival

$$\Delta S_{\text{all}}(t_i) = S_{\text{all}}(t_{i-1}) - S_{\text{all}}(t_i) = \Delta\text{CIF}_{i,T} + \Delta\text{CIF}_{i,C}. \quad (76)$$

The classical CGE assumes that at each t_i only one of the two increments is non-zero, $\Delta\text{CIF}_{i,T} \cdot \Delta\text{CIF}_{i,C} = 0$, so that the decrease in Eq. 76 can be attributed to exactly one cause at each step. Under this assumption, the recursion proceeds as follows. Suppose $\Delta\text{CIF}_{i,T} > 0$ and $\Delta\text{CIF}_{i,C} = 0$. Then the event occurs within $(t_{i-1}, t_i]$ among those still in the joint risk set, and we have that

$$G(t_i) = G(t_{i-1}), \quad S_{\text{all}}(t_i) = S_{\text{all}}(t_{i-1}) - \Delta\text{CIF}_{i,T}. \quad (77)$$

Plugging into Eq. 74 yields an explicit update for $S(t_i)$:

$$\varphi^{-1}\left(\varphi(S_{\text{all}}(t_i)) - \varphi(G(t_{i-1}))\right). \quad (78)$$

Analogously, if $\Delta\text{CIF}_{i,C} > 0$ and $\Delta\text{CIF}_{i,T} = 0$, then $S(t_i) = S(t_{i-1})$ and

$$G(t_i) = \varphi^{-1}\left(\varphi(S_{\text{all}}(t_i)) - \varphi(S(t_{i-1}))\right). \quad (79)$$

Thus, given $\{S_{\text{all}}(t_i), \text{CIF}_T(t_i), \text{CIF}_C(t_i)\}_{i=0}^m$ (which are estimable from the data even under informative censoring) and the single-jump assumption, the recursion in Eqs. 78-79 identifies the marginal survivals (S, G) for a fixed τ .

Bounds when both increments may be non-zero. In our setting, CIF_T and CIF_C are available only on a fixed grid of estimates, and we cannot assume $\Delta\text{CIF}_{i,T} \cdot \Delta\text{CIF}_{i,C} = 0$. Consequently, Eq. 74 together with $S_{\text{all}}(t_i)$ does not uniquely determine $(S(t_i), G(t_i))$ from $(S(t_{i-1}), G(t_{i-1}))$. Thm. 3 below gives sharp one-step lower and upper bounds implied by Eq. 74, generalizing the classical recursion of Eqs. (78) and (79) to the non-disjoint case. To state it, define the marginal decrease candidates

$$H(t_{i-1}, t_i) = S_{\text{all}}(t_{i-1}) - \Delta\text{CIF}_{i,C} = S_{\text{all}}(t_i) + \Delta\text{CIF}_{i,T}, \quad (80)$$

$$H(t_i, t_{i-1}) = S_{\text{all}}(t_{i-1}) - \Delta\text{CIF}_{i,T} = S_{\text{all}}(t_i) + \Delta\text{CIF}_{i,C}. \quad (81)$$

Intuitively, events T, C *compete* for individuals in the risk set in $(t_{i-1}, t_i]$. The value $H(t_{i-1}, t_i)$ corresponds to the configuration in which the censoring proportion in $(t_{i-1}, t_i]$ would be unchanged in the absence of competition from T , yielding the upper bound for $G(t_i)$ and lower bound for $S(t_i)$. Conversely, $H(t_i, t_{i-1})$ holds the event proportion fixed in the absence of censoring, yielding the upper bound on $S(t_i)$ and lower bound on $G(t_i)$.

Theorem 3 (CGE bounds under non-disjoint increments). *Let φ be an Archimedean copula generator and assume $H(t, c) = C_T(S(t), G(c))$ on $[t_{i-1}, t_i]$. Given $(S(t_{i-1}), G(t_{i-1}))$ and the increments $\Delta\text{CIF}_{i,T}, \Delta\text{CIF}_{i,C} \geq 0$ with $S_{\text{all}}(t_i) = S_{\text{all}}(t_{i-1}) - \Delta\text{CIF}_{i,T} - \Delta\text{CIF}_{i,C}$, the marginals at t_i satisfy $S(t_i) \in [\underline{S}(t_i), \overline{S}(t_i)]$ and $G(t_i) \in [\underline{G}(t_i), \overline{G}(t_i)]$, where*

$$\overline{G}(t_i) = \varphi^{-1}(\varphi(H(t_{i-1}, t_i)) - \varphi(S(t_{i-1}))), \quad (82)$$

$$\underline{S}(t_i) = \varphi^{-1}(\varphi(S_{\text{all}}(t_i)) - \varphi(\overline{G}(t_i))), \quad (83)$$

$$\overline{S}(t_i) = \varphi^{-1}(\varphi(H(t_i, t_{i-1})) - \varphi(G(t_{i-1}))), \quad (84)$$

$$\underline{G}(t_i) = \varphi^{-1}(\varphi(S_{\text{all}}(t_i)) - \varphi(\overline{S}(t_i))), \quad (85)$$

with $H(t_{i-1}, t_i) = S_{\text{all}}(t_{i-1}) - \Delta\text{CIF}_{i,C}$ and $H(t_i, t_{i-1}) = S_{\text{all}}(t_{i-1}) - \Delta\text{CIF}_{i,T}$. The bounds are sharp, and as $\max_i |t_i - t_{i-1}| \rightarrow 0$ they collapse, point-identifying (S, G) for fixed τ . \square

Proof. By Eq. 74, $\varphi(H(t, c)) = \varphi(S(t)) + \varphi(G(c))$ for all (t, c) in the interval. Evaluating at (t_{i-1}, t_i) gives

$$\varphi(G(t_i)) = \varphi(H(t_{i-1}, t_i)) - \varphi(S(t_{i-1})),$$

where $G(t_i)$ is maximized when $H(t_{i-1}, t_i)$ takes its largest admissible value, namely $S_{\text{all}}(t_{i-1}) - \Delta\text{CIF}_{i,C}$ (corresponding to attributing the full censoring increment to C alone in $(t_{i-1}, t_i]$, while ascribing none of the joint decrease to T over and above what is forced). This yields $\overline{G}(t_i)$ (since φ is strictly decreasing). The companion lower bound $\underline{S}(t_i)$ follows by enforcing the additive identity $\varphi(S_{\text{all}}(t_i)) = \varphi(S(t_i)) + \varphi(G(t_i))$ and substituting $\overline{G}(t_i)$. The pair $(\overline{S}(t_i), \underline{G}(t_i))$ is obtained by the symmetric argument starting from $H(t_i, t_{i-1})$. For sharpness, we note each extremum is attained by the limiting configuration in which one cause's increment is realized first within $(t_{i-1}, t_i]$, recovering the classical single-jump recursion of Eqs. (78) and (79). For point collapse, observe that when $\Delta\text{CIF}_{i,T} = 0$, update (ii) yields $\overline{S}(t_i) = S(t_{i-1})$ via the additive identity $\varphi(S_{\text{all}}(t_{i-1})) = \varphi(S(t_{i-1})) + \varphi(G(t_{i-1}))$, and update (i) then determines $G(t_i)$ uniquely; the bounds coincide and reduce to the classical recursion of Eqs. (78) and (79). The symmetric argument applies when $\Delta\text{CIF}_{i,C} = 0$. Hence under, any grid refinement finer than the minimum gap between jump times of CIF_T and CIF_C (pairwise distinct when T, C are continuously distributed), each interval contains at most one increment, and the bounds collapse. \square

In practice, from these bounds we extract the midpoints as our estimates

$$\hat{S}(t_i) = \frac{1}{2}(\underline{S}(t_i) + \overline{S}(t_i)), \quad \hat{G}(t_i) = \frac{1}{2}(\underline{G}(t_i) + \overline{G}(t_i)), \quad (86)$$

and iterate forward in i .

D.1 Uncertainty Envelope

The above description provides the copula-graphic mapping from cumulative incidence functions to the marginal survival curves. In the case where uncertainty quantification is available over the CIFs (e.g., when doubly robust estimation is performed), the key challenge is to propagate the uncertainty in the CIFs into the marginal survival curve uncertainty. We now discuss the method for doing so.

Corner evaluation. A natural first approximation is to evaluate the copula-graphic estimator at the four extremal combinations of lower and upper CIF $(1 - \alpha)$ -confidence intervals,

$$(\underline{\text{CIF}}_T, \underline{\text{CIF}}_C), \quad (\underline{\text{CIF}}_T, \overline{\text{CIF}}_C), \quad (\overline{\text{CIF}}_T, \underline{\text{CIF}}_C), \quad (\overline{\text{CIF}}_T, \overline{\text{CIF}}_C),$$

and to take the pointwise minima and maxima of the resulting survival curves as an uncertainty envelope. While simple and inexpensive, this approach does not provide a formal guarantee of capturing the true extrema, since the copula-graphic map need not be jointly monotone in the CIF arguments.

Sampling-based envelope. To obtain a more reliable envelope, we augment the corner evaluation with a sampling step over the admissible CIF region circumscribed by its $(1 - \alpha)$ -confidence interval. After estimating lower and upper bounds for CIF_T and CIF_C , we repeatedly draw CIF trajectories uniformly within these bands on the time grid, and ensure each draw is a valid CIF by enforcing (i)

non-negativity, (ii) non-negative increments, and (iii) the pointwise constraint $\text{CIF}_T(t) + \text{CIF}_C(t) \leq 1$. For each sampled pair, we apply the copula-graphic recursion to obtain a candidate survival curve. The final uncertainty envelope is then defined by the pointwise minima and maxima over the survival curves obtained from the four corners together with the sampled trajectories, and these confidence intervals are reported in practice (see Fig. 4).

E ANZICS Acknowledgement

The authors acknowledge the Australian and New Zealand Intensive Care Society (ANZICS) Centre for Outcomes and Resource Evaluation (CORE) for providing the data used in the current study. The authors and the management committee of ANZICS CORE would like to thank clinicians, data collectors and researchers at the following contributing sites:

| |
|---|
| Albury Wodonga Health ICU |
| Alfred Hospital ICU |
| Alice Springs Hospital ICU |
| Allamanda Private Hospital ICU |
| Angliss Hospital ICU |
| Armadale Health Service ICU |
| Ashford Community Hospital ICU |
| Auckland City Hospital CV ICU |
| Auckland City Hospital DCCM |
| Austin Hospital ICU |
| Ballarat Health Services ICU |
| Bankstown-Lidcombe Hospital ICU |
| Bathurst Base Hospital ICU |
| Bendigo Health Care Group ICU |
| Blacktown Hospital ICU |
| Bowral Hospital HDU |
| Box Hill Hospital ICU |
| Braemar Hospital SCU |
| Brisbane Private Hospital ICU |
| Brisbane Waters Private Hospital ICU |
| Broken Hill Base Hospital & Health Services ICU |
| Buderim Private Hospital ICU |
| Bunbury Regional Hospital ICU |
| Bundaberg Base Hospital ICU |
| Caboolture Hospital ICU |
| Cabrini Hospital ICU |
| Cairns Hospital ICU |
| Calvary Adelaide Hospital ICU |
| Calvary Bruce Private Hospital HDU |
| Calvary Hospital (Canberra) ICU |
| Calvary Hospital (Lenah Valley) ICU |
| Calvary John James Hospital ICU |
| Calvary Mater Newcastle ICU |
| Calvary North Adelaide Hospital ICU |
| Campbelltown Hospital ICU |
| Canberra Hospital ICU |
| Casey Hospital ICU |
| Central Gippsland Health Service (Sale) ICU |
| Christchurch Hospital ICU |
| Coffs Harbour Health Campus ICU |
| Concord Hospital (Sydney) ICU |
| Dandenong Hospital ICU |
| Dubbo Base Hospital ICU |
| Dunedin Hospital ICU |
| Echuca Regional Hospital HDU |
| Epworth Eastern Private Hospital ICU |
| Epworth Freemasons Hospital ICU |
| Epworth Geelong ICU |
| Epworth Hospital (Richmond) ICU |
| Fairfield Hospital ICU |

| |
|--|
| Fiona Stanley Hospital ICU |
| Flinders Medical Centre ICU |
| Flinders Private Hospital ICU |
| Footscray Hospital ICU |
| Frankston Hospital ICU |
| Fremantle Hospital ICU |
| Gold Coast Private Hospital ICU |
| Gold Coast University Hospital ICU |
| Gosford Hospital ICU |
| Gosford Private Hospital ICU |
| Goulburn Base Hospital ICU |
| Goulburn Valley Health ICU |
| Grafton Base Hospital ICU |
| Greenslopes Private Hospital ICU |
| Griffith Base Hospital ICU |
| Hawkes Bay Hospital ICU |
| Hervey Bay Hospital ICU |
| Hollywood Private Hospital ICU |
| Holmesglen Private Hospital ICU |
| Hornsby Ku-ring-gai Hospital ICU |
| Hurstville Private Hospital ICU |
| Hutt Hospital ICU |
| Ipswich Hospital ICU |
| John Fawcner Hospital ICU |
| John Hunter Hospital ICU |
| Joondalup Health Campus ICU |
| Kareena Private Hospital ICU |
| Knox Private Hospital ICU |
| Latrobe Regional Hospital ICU |
| Launceston General Hospital ICU |
| Lingard Private Hospital ICU |
| Lismore Base Hospital ICU |
| Liverpool Hospital ICU |
| Logan Hospital ICU |
| Lyell McEwin Hospital ICU |
| Mackay Base Hospital ICU |
| Macquarie University Private Hospital ICU |
| Maitland Hospital ICU |
| Maitland Private Hospital ICU |
| Manly Hospital & Community Health ICU |
| Manning Rural Referral Hospital ICU |
| Maroondah Hospital ICU |
| Mater Adults Hospital (Brisbane) ICU |
| Mater Health Services North Queensland ICU |
| Mater Private Hospital (Brisbane) ICU |
| Mater Private Hospital (Sydney) ICU |
| Melbourne Private Hospital ICU |
| Middlemore Hospital ICU |
| Mildura Base Public Hospital ICU |
| Modbury Public Hospital ICU |
| Monash Medical Centre-Clayton Campus ICU |
| Mount Hospital ICU |
| Mount Isa Hospital ICU |
| Mulgrave Private Hospital ICU |
| Nambour General Hospital ICU |
| National Capital Private Hospital ICU |

| |
|---|
| Nelson Hospital ICU |
| Nepean Hospital ICU |
| Nepean Private Hospital ICU |
| Newcastle Private Hospital ICU |
| Noosa Hospital ICU |
| North Shore Hospital ICU |
| North Shore Private Hospital ICU |
| North West Private Hospital ICU |
| North West Regional Hospital (Burnie) ICU |
| Northeast Health Wangaratta ICU |
| Northern Beaches Hospital ICU |
| Norwest Private Hospital ICU |
| Orange Base Hospital ICU |
| Peninsula Private Hospital ICU |
| Peter MacCallum Cancer Institute ICU |
| Pindara Private Hospital ICU |
| Port Macquarie Base Hospital ICU |
| Prince of Wales Hospital (Hong Kong) ICU |
| Prince of Wales Hospital (Sydney) ICU |
| Prince of Wales Private Hospital (Sydney) ICU |
| Princess Alexandra Hospital ICU |
| Queen Elizabeth II Jubilee Hospital ICU |
| Redcliffe Hospital ICU |
| Robina Hospital ICU |
| Rockhampton Hospital ICU |
| Rockingham General Hospital ICU |
| Rotorua Hospital ICU |
| Royal Adelaide Hospital ICU |
| Royal Brisbane and Women's Hospital ICU |
| Royal Darwin Hospital ICU |
| Royal Hobart Hospital ICU |
| Royal Melbourne Hospital ICU |
| Royal North Shore Hospital ICU |
| Royal Perth Hospital ICU |
| Royal Prince Alfred Hospital ICU |
| Ryde Hospital and Community Health Services ICU |
| Shoalhaven Hospital ICU |
| Sir Charles Gairdner Hospital ICU |
| South East Regional Hospital ICU |
| South West Healthcare (Warrnambool) ICU |
| Southern Cross Hospital (Hamilton) ICU |
| Southern Cross Hospital (Wellington) ICU |
| St Andrew's Hospital Toowoomba ICU |
| St Andrew's Private Hospital (Ipswich) ICU |
| St Andrew's War Memorial Hospital ICU |
| St George Hospital (Sydney) CICU |
| St George Hospital (Sydney) ICU |
| St George Hospital (Sydney) ICU2 |
| St George Private Hospital (Sydney) ICU |
| St John Of God Health Care (Subiaco) ICU |
| St John Of God Hospital (Ballarat) ICU |
| St John of God Hospital (Bendigo) ICU |
| St John of God Hospital (Berwick) ICU |
| St John Of God Hospital (Geelong) ICU |
| St John of God Midland Public & Private ICU |
| St Vincent's Private Hospital Northside ICU |

| |
|---|
| St Vincent's Hospital (Melbourne) ICU |
| St Vincent's Hospital (Sydney) ICU |
| St Vincent's Hospital (Toowoomba) ICU |
| St Vincent's Private Hospital (Sydney) ICU |
| St Vincent's Private Hospital Fitzroy ICU |
| Sunnybank Hospital ICU |
| Sunshine Coast University Hospital ICU |
| Sunshine Coast University Private Hospital ICU |
| Sunshine Hospital ICU |
| Sutherland Hospital & Community Health Services ICU |
| Sydney Adventist Hospital ICU |
| Tamworth Base Hospital ICU |
| Taranaki Health ICU |
| Tauranga Hospital ICU |
| The Bays Hospital ICU |
| The Chris O'Brien Lifehouse ICU |
| The Memorial Hospital (Adelaide) ICU |
| The Northern Hospital ICU |
| The Prince Charles Hospital ICU |
| The Queen Elizabeth (Adelaide) ICU |
| The Wesley Hospital ICU |
| Timaru Hospital ICU |
| Toowoomba Hospital ICU |
| Townsville University Hospital ICU |
| Tweed Heads District Hospital ICU |
| University Hospital Geelong ICU |
| Wagga Wagga Base Hospital & District Health ICU |
| Waikato Hospital ICU |
| Wairau Hospital ICU |
| Warringal Private Hospital ICU |
| Wellington Hospital ICU |
| Werribee Mercy Hospital ICU |
| Western District Health Service (Hamilton) ICU |
| Western Hospital (SA) ICU |
| Western Private Hospital ICU |
| Westmead Hospital ICU |
| Westmead Private Hospital ICU |
| Whangarei Area Hospital - Northland Health Ltd ICU |
| Wimmera Health Care Group (Horsham) ICU |
| Wollongong Hospital ICU |
| Women's and Children's Hospital PICU |
| Wyong Hospital ICU |